Third Edition

Sponsored by the Optical Society of America

HANDBOOK OF OPTICS

Volume II

Design, Fabrication, and Testing; Sources and Detectors; Radiometry and Photometry

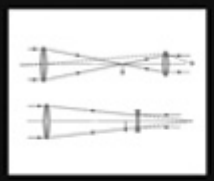

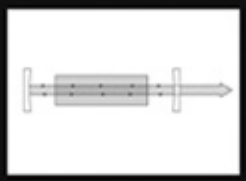

Editor-in-Chief:
Michael Bass

Associate Editors:
Casimer M. DeCusatis
Jay M. Enoch
Vasudevan Lakshminarayanan
Guifang Li
Carolyn MacDonald
Virendra N. Mahajan
Eric Van Stryland

OSA

SPERO EX. 2051

HANDBOOK OF OPTICS

SPERO EX. 2051

ABOUT THE EDITORS

Editor-in-Chief: Dr. Michael Bass is professor emeritus at CREOL, The College of Optics and Photonics, University of Central Florida, Orlando, Florida.

Associate Editors:
Dr. Casimer M. DeCusatis is a distinguished engineer and technical executive with IBM Corporation.

Dr. Jay M. Enoch is dean emeritus and professor at the School of Optometry at the University of California, Berkeley.

Dr. Vasudevan Lakshminarayanan is professor of Optometry, Physics, and Electrical Engineering at the University of Waterloo, Ontario, Canada.

Dr. Guifang Li is a professor at CREOL, The College of Optics and Photonics, University of Central Florida, Orlando, Florida.

Dr. Carolyn MacDonald is a professor at the University at Albany, and director of the Center for X-Ray Optics.

Dr. Virendra N. Mahajan is a distinguished scientist at The Aerospace Corporation.

Dr. Eric Van Stryland is a professor at CREOL, The College of Optics and Photonics, University of Central Florida, Orlando, Florida.

SPERO EX. 2051

HANDBOOK OF OPTICS

Volume II
Design, Fabrication, and Testing;
Sources and Detectors;
Radiometry and Photometry

THIRD EDITION

Sponsored by the
OPTICAL SOCIETY OF AMERICA

Michael Bass Editor-in-Chief
CREOL, The College of Optics and Photonics
University of Central Florida
Orlando, Florida

Virendra N. Mahajan Associate Editor
The Aerospace Corporation
El Segundo, California

Eric Van Stryland Associate Editor
CREOL, The College of Optics and Photonics
University of Central Florida
Orlando, Florida

New York Chicago San Francisco Lisbon London Madrid
Mexico City Milan New Delhi San Juan Seoul
Singapore Sydney Toronto

SPERO EX. 2051

The McGraw·Hill Companies

Copyright © 2010 by The McGraw-Hill Companies, Inc. All rights reserved. Except as permitted under the United States Copyright Act of 1976, no part of this publication may be reproduced or distributed in any form or by any means, or stored in a database or retrieval system, without the prior written permission of the publisher.

ISBN 978-0-07162927-0, MHID 0-07-162927-0

The material in this eBook also appears in the print version of this title. ISBN: P/N 978-0-07-163600-1 of set 978-0-07-149890-6. MHID: P/N 0-07-163600-5 of set 0-07-149890-7.

All trademarks are trademarks of their respective owners. Rather than put a trademark symbol after every occurrence of a trademarked name, we use names in an editorial fashion only, and to the benefit of the trademark owner, with no intention of infringement of the trademark. Where such designations appear in this book, they have been printed with initial caps.

McGraw-Hill eBooks are available at special quantity discounts to use as premiums and sales promotions, or for use in corporate training programs. To contact a representative please e-mail us at bulksales@mcgraw-hill.com.

TERMS OF USE

This is a copyrighted work and The McGraw-Hill Companies, Inc. ("McGraw-Hill") and its licensors reserve all rights in and to the work. Use of this work is subject to these terms. Except as permitted under the Copyright Act of 1976 and the right to store and retrieve one copy of the work, you may not decompile, disassemble, reverse engineer, reproduce, modify, create derivative works based upon, transmit, distribute, disseminate, sell, publish or sublicense the work or any part of it without McGraw-Hill's prior consent. You may use the work for your own noncommercial and personal use; any other use of the work is strictly prohibited. Your right to use the work may be terminated if you fail to comply with these terms.

THE WORK IS PROVIDED "AS IS." McGRAW-HILL AND ITS LICENSORS MAKE NO GUARANTEES OR WARRANTIES AS TO THE ACCURACY, ADEQUACY OR COMPLETENESS OF OR RESULTS TO BE OBTAINED FROM USING THE WORK, INCLUDING ANY INFORMATION THAT CAN BE ACCESSED THROUGH THE WORK VIA HYPERLINK OR OTHERWISE, AND EXPRESSLY DISCLAIM ANY WARRANTY, EXPRESS OR IMPLIED, INCLUDING BUT NOT LIMITED TO IMPLIED WARRANTIES OF MERCHANTABILITY OR FITNESS FOR A PARTICULAR PURPOSE. McGraw-Hill and its licensors do not warrant or guarantee that the functions contained in the work will meet your requirements or that its operation will be uninterrupted or error free. Neither McGraw-Hill nor its licensors shall be liable to you or anyone else for any inaccuracy, error or omission, regardless of cause, in the work or for any damages resulting therefrom. McGraw-Hill has no responsibility for the content of any information accessed through the work. Under no circumstances shall McGraw-Hill and/or its licensors be liable for any indirect, incidental, special, punitive, consequential or similar damages that result from the use of or inability to use the work, even if any of them has been advised of the possibility of such damages. This limitation of liability shall apply to any claim or cause whatsoever whether such claim or cause arises in contract, tort or otherwise.

Information contained in this work has been obtained by The McGraw-Hill Companies, Inc. ("McGraw-Hill") from sources believed to be reliable. However, neither McGraw-Hill nor its authors guarantee the accuracy or completeness of any information published herein, and neither McGraw-Hill nor its authors shall be responsible for any errors, omissions, or damages arising out of use of this information. This work is published with the understanding that McGraw-Hill and its authors are supplying information but are not attempting to render engineering or other professional services. If such services are required, the assistance of an appropriate professional should be sought.

SPERO EX. 2051

COVER ILLUSTRATIONS

Left: Telescope such as used by Galileo to discover lunar craters and Jupiter's moons. The basic design is still used in opera and sports glasses. See Chap. 1.

Middle: Simplified schematic of a laser showing the gain medium which amplifies the light, and the resonator which defines the light's direction and spatial distribution. The third critical part, the source to excite the gain medium, is not shown. See Chap. 16.

Right: Zernike circle polynomial representing balanced astigmatism with a standard deviation of one wave illustrated as an isometric plot on the top, interferogram on the left, and point-spread function on the right. See Chap. 11.

SPERO EX. 2051

This page intentionally left blank.

CONTENTS

Contributors xvii
Brief Contents of All Volumes xix
Editors' Preface xxv
Preface to Volume II xxvii
Glossary and Fundamental Constants xxix

Part 1. Design

Chapter 1. Techniques of First-Order Layout *Warren J. Smith* 1.3

1.1 Glossary / *1.3*
1.2 First-Order Layout / *1.4*
1.3 Ray-Tracing / *1.4*
1.4 Two-Component Systems / *1.5*
1.5 Afocal Systems / *1.7*
1.6 Magnifiers and Microscopes / *1.8*
1.7 Afocal Attachments / *1.8*
1.8 Field Lenses / *1.8*
1.9 Condensers / *1.10*
1.10 Zoom or Varifocal Systems / *1.11*
1.11 Additional Rays / *1.12*
1.12 Minimizing Component Power / *1.13*
1.13 Is It a Reasonable Layout? / *1.13*
1.14 Achromatism / *1.14*
1.15 Athermalization / *1.15*

Chapter 2. Aberration Curves in Lens Design *Donald C. O'Shea and Michael E. Harrigan* 2.1

2.1 Glossary / *2.1*
2.2 Introduction / *2.1*
2.3 Transverse Ray Plots / *2.2*
2.4 Field Plots / *2.4*
2.5 Additional Considerations / *2.5*
2.6 Summary / *2.6*
2.7 References / *2.6*

Chapter 3. Optical Design Software *Douglas C. Sinclair* 3.1

3.1 Glossary / *3.1*
3.2 Introduction / *3.2*
3.3 Lens Entry / *3.2*
3.4 Evaluation / *3.8*
3.5 Optimization / *3.16*
3.6 Other Topics / *3.21*
3.7 Buying Optical Design Software / *3.22*
3.8 Summary / *3.24*
3.9 References / *3.24*

SPERO EX. 2051

Chapter 4. Optical Specifications *Robert R. Shannon* 4.1

4.1 Glossary / *4.1*
4.2 Introduction / *4.1*
4.3 Preparation of Optical Specifications / *4.5*
4.4 Image Specifications / *4.6*
4.5 Element Description / *4.8*
4.6 Environmental Specifications / *4.10*
4.7 Presentation of Specifications / *4.10*
4.8 Problems with Specification Writing / *4.11*
4.9 References / *4.12*

Chapter 5. Tolerancing Techniques *Robert R. Shannon* 5.1

5.1 Glossary / *5.1*
5.2 Introduction / *5.1*
5.3 Wavefront Tolerances / *5.3*
5.4 Other Tolerances / *5.7*
5.5 Starting Points / *5.8*
5.6 Material Properties / *5.9*
5.7 Tolerancing Procedures / *5.9*
5.8 Problems in Tolerancing / *5.11*
5.9 References / *5.11*

Chapter 6. Mounting Optical Components *Paul R. Yoder, Jr.* 6.1

6.1 Glossary / *6.1*
6.2 Introduction and Summary / *6.1*
6.3 Mounting Individual Rotationally Symmetric Optics / *6.2*
6.4 Multicomponent Lens Assemblies / *6.5*
6.5 Mounting Windows and Domes / *6.11*
6.6 Mounting Small Mirrors and Prisms / *6.11*
6.7 Mounting Moderate-Sized Mirrors / *6.17*
6.8 Contact Stresses in Optics / *6.21*
6.9 Temperature Effects on Mounted Optics / *6.21*
6.10 References / *6.25*

Chapter 7. Control of Stray Light *Robert P. Breault* 7.1

7.1 Glossary / *7.1*
7.2 Introduction / *7.1*
7.3 Concepts / *7.2*
7.4 Optical Software for Stray Light Analysis / *7.24*
7.5 Methods / *7.27*
7.6 Conclusion / *7.30*
7.7 Sources of Information on Stray Light and Scattered Light / *7.31*
7.8 References / *7.32*

Chapter 8. Thermal Compensation Techniques *Philip J. Rogers and Michael Roberts* 8.1

8.1 Glossary / *8.1*
8.2 Introduction / *8.2*
8.3 Homogeneous Thermal Effects / *8.2*
8.4 Tolerable Homogeneous Temperature Change (No Compensation) / *8.5*
8.5 Effect of Thermal Gradients / *8.6*
8.6 Intrinsic Athermalization / *8.7*
8.7 Mechanical Athermalization / *8.8*
8.8 Optical Athermalization / *8.12*
8.9 References / *8.15*

SPERO EX. 2051

Part 2. Fabrication

Chapter 9. Optical Fabrication *Michael P. Mandina* 9.3

9.1 Introduction / *9.3*
9.2 Material Forms of Supply / *9.3*
9.3 Basic Steps in Spherical Optics Fabrication / *9.4*
9.4 Plano Optics Fabrication / *9.7*
9.5 Asphere Optics Fabrication / *9.7*
9.6 Crystalline Optics / *9.8*
9.7 Purchasing Optics / *9.9*
9.8 Conclusion / *9.9*
9.9 References / *9.9*

Chapter 10. Fabrication of Optics by Diamond Turning *Richard L. Rhorer and Chris J. Evans* 10.1

10.1 Glossary / *10.1*
10.2 Introduction / *10.1*
10.3 The Diamond-Turning Process / *10.2*
10.4 The Advantages of Diamond Turning / *10.2*
10.5 Diamond-Turnable Materials / *10.4*
10.6 Comparison of Diamond Turning and Traditional Optical Fabrication / *10.6*
10.7 Machine Tools for Diamond Turning / *10.6*
10.8 Basic Steps in Diamond Turning / *10.8*
10.9 Surface Finish of Diamond-Turned Optics / *10.9*
10.10 Metrology of Diamond-Turned Optics / *10.12*
10.11 Conclusions / *10.13*
10.12 References / *10.14*

Part 3. Testing

Chapter 11. Orthonormal Polynomials in Wavefront Analysis *Virendra N. Mahajan* 11.3

Abstract / *11.3*
11.1 Glossary / *11.3*
11.2 Introduction / *11.4*
11.3 Orthonormal Polynomials / *11.5*
11.4 Zernike Circle Polynomials / *11.6*
11.5 Zernike Annular Polynomials / *11.13*
11.6 Hexagonal Polynomials / *11.21*
11.7 Elliptical Polynomials / *11.21*
11.8 Rectangular Polynomials / *11.27*
11.9 Square Polynomials / *11.30*
11.10 Slit Polynomials / *11.30*
11.11 Aberration Balancing and Tolerancing, and Diffraction Focus / *11.30*
11.12 Isometric, Interferometric, and PSF Plots for Orthonormal Aberrations / *11.36*
11.13 Use of Circle Polynomials for Noncircular Pupils / *11.37*
11.14 Discussion and Conclusions / *11.39*
11.15 References / *11.40*

Chapter 12. Optical Metrology *Zacarías Malacara and Daniel Malacara-Hernández* 12.1

12.1 Glossary / *12.1*
12.2 Introduction and Definitions / *12.2*

SPERO EX. 2051

12.3 Length and Straightness Measurements / *12.2*
12.4 Angle Measurements / *12.10*
12.5 Curvature and Focal Length Measurements / *12.17*
12.6 References / *12.25*

Chapter 13. Optical Testing *Daniel Malacara-Hernández* 13.1

13.1 Glossary / *13.1*
13.2 Introduction / *13.1*
13.3 Classical Noninterferometric Tests / *13.1*
13.4 Interferometric Tests / *13.7*
13.5 Increasing the Sensitivity of Interferometers / *13.13*
13.6 Interferogram Evaluation / *13.14*
13.7 Phase-Shifting Interferometry / *13.18*
13.8 Measuring Aspherical Wavefronts / *13.23*
13.9 References / *13.28*

Chapter 14. Use of Computer-Generated Holograms in Optical Testing *Katherine Creath and James C. Wyant* 14.1

14.1 Glossary / *14.1*
14.2 Introduction / *14.1*
14.3 Plotting CGHs / *14.3*
14.4 Interferometers Using Computer-Generated Holograms / *14.4*
14.5 Accuracy Limitations / *14.6*
14.6 Experimental Results / *14.7*
14.7 Discussion / *14.9*
14.8 References / *14.9*

Part 4. Sources

Chapter 15. Artificial Sources *Anthony LaRocca* 15.3

15.1 Glossary / *15.3*
15.2 Introduction / *15.3*
15.3 Radiation Law / *15.4*
15.4 Laboratory Sources / *15.7*
15.5 Commercial Sources / *15.13*
15.6 References / *15.53*

Chapter 16. Lasers *William T. Silfvast* 16.1

16.1 Glossary / *16.1*
16.2 Introduction / *16.2*
16.3 Laser Properties Associated with the Laser Gain Medium / *16.4*
16.4 Laser Properties Associated with Optical Cavities or Resonators / *16.19*
16.5 Special Laser Cavities / *16.25*
16.6 Specific Types of Lasers / *16.29*
16.7 References / *16.37*

Chapter 17. Light-Emitting Diodes *Roland H. Haitz, M. George Craford, and Robert H. Weissman* 17.1

17.1 Glossary / *17.1*
17.2 Introduction / *17.2*
17.3 Light-Generation Processes / *17.2*
17.4 Light Extraction / *17.6*
17.5 Device Structures / *17.8*

SPERO EX. 2051

17.6 Material Systems / *17.15*
17.7 Substrate Technology / *17.20*
17.8 Epitaxial Technology / *17.21*
17.9 Wafer Processing / *17.23*
17.10 Led Quality and Reliability / *17.25*
17.11 Led-Based Products / *17.29*
17.12 References / *17.35*

Chapter 18. High-Brightness Visible LEDs *Winston V. Schoenfeld* 18.1

18.1 The Materials Systems / *18.1*
18.2 Substrates and Epitaxial Growth / *18.2*
18.3 Processing / *18.3*
18.4 Solid-State Lighting / *18.4*
18.5 Packaging / *18.5*

Chapter 19. Semiconductor Lasers *Pamela L. Derry, Luis Figueroa, and Chi-Shain Hong* 19.1

19.1 Glossary / *19.1*
19.2 Introduction / *19.3*
19.3 Applications for Semiconductor Lasers / *19.3*
19.4 Basic Operation / *19.4*
19.5 Fabrication and Configurations / *19.6*
19.6 Quantum Well Lasers / *19.9*
19.7 High-Power Semiconductor Lasers / *19.18*
19.8 High-Speed Modulation / *19.30*
19.9 Spectral Properties / *19.36*
19.10 Surface-Emitting Lasers / *19.39*
19.11 Conclusion / *19.41*
19.12 References / *19.43*

Chapter 20. Ultrashort Optical Sources and Applications *Jean-Claude Diels and Ladan Arissian* 20.1

20.1 Introduction / *20.1*
20.2 Description of Optical Pulses and Pulse Trains / *20.2*
20.3 Pulse Evolution toward Steady State / *20.9*
20.4 Coupling Circulating Pulses Inside a Cavity / *20.12*
20.5 Designs of Cavities with Two Circulating Pulses / *20.15*
20.6 Analogy of a Two-Level System / *20.22*
20.7 Conclusion / *20.28*
20.8 References / *20.28*

Chapter 21. Attosecond Optics *Zenghu Chang* 21.1

21.1 Glossary / *21.1*
21.2 Introduction / *21.2*
21.3 The Driving Laser / *21.4*
21.4 Attosecond Pulse Generation / *21.6*
21.5 Attosecond Pulse Characterization / *21.8*
21.6 Acknowledgments / *21.10*
21.7 References / *21.10*

Chapter 22. Laser Stabilization *John L. Hall, Matthew S. Taubman, and Jun Ye* 22.1

22.1 Introduction and Overview / *22.1*
22.2 Servo Principles and Issues / *22.5*

SPERO EX. 2051

22.3 Practical Issues / *22.12*
22.4 Summary and Outlook / *22.23*
22.5 Conclusions and Recommendations / *22.24*
22.6 Acknowledgments / *22.24*
22.7 References / *22.24*

Chapter 23. Quantum Theory of the Laser *János A. Bergou, Berthold-Georg Englert, Melvin Lax, Marian O. Scully, Herbert Walther, and M. Suhail Zubairy* 23.1

23.1 Glossary / *23.1*
23.2 Introduction / *23.5*
23.3 Some History of the Photon Concept / *23.6*
23.4 Quantum Theory of the Laser / *23.14*
23.5 The Laser Phase-Transition Analogy / *23.35*
23.6 Exotic Masers and Lasers / *23.40*
23.7 Acknowledgments / *23.45*
23.8 References / *23.46*

Part 5. Detectors

Chapter 24. Photodetectors *Paul R. Norton* 24.3

24.1 Scope / *24.3*
24.2 Thermal Detectors / *24.4*
24.3 Quantum Detectors / *24.6*
24.4 Definitions / *24.10*
24.5 Detector Performance and Sensitivity / *24.13*
24.6 Other Performance Parameters / *24.18*
24.7 Detector Performance / *24.21*
24.8 References / *24.101*
24.9 Suggested Readings / *24.102*

Chapter 25. Photodetection *Abhay M. Joshi and Gregory H. Olsen* 25.1

25.1 Glossary / *25.1*
25.2 Introduction / *25.2*
25.3 Principle of Operation / *25.3*
25.4 Applications / *25.11*
25.5 Reliability / *25.13*
25.6 Future Photodetectors / *25.15*
25.7 Acknowledgment / *25.17*
25.8 References / *25.18*
25.9 Additional Reading / *25.19*

Chapter 26. High-Speed Photodetectors *J. E. Bowers and Y. G. Wey* 26.1

26.1 Glossary / *26.1*
26.2 Introduction / *26.3*
26.3 Photodetector Structures / *26.3*
26.4 Speed Limitations / *26.5*
26.5 *p-i-n* Photodetectors / *26.10*
26.6 Schottky Photodiode / *26.16*
26.7 Avalanche Photodetectors / *26.17*
26.8 Photoconductors / *26.20*

SPERO EX. 2051

26.9 Summary / *26.24*
26.10 References / *26.24*

Chapter 27. Signal Detection and Analysis *John R. Willison* 27.1

27.1 Glossary / *27.1*
27.2 Introduction / *27.1*
27.3 Prototype Experiment / *27.2*
27.4 Noise Sources / *27.3*
27.5 Applications Using Photomultipliers / *27.6*
27.6 Amplifiers / *27.10*
27.7 Signal Analysis / *27.12*
27.8 References / *27.15*

Chapter 28. Thermal Detectors *William L. Wolfe and Paul W. Kruse* 28.1

28.1 Glossary / *28.1*
28.2 Thermal Detector Elements / *28.1*
28.3 Arrays / *28.7*
28.4 References / *28.13*

Part 6. Imaging Detectors

Chapter 29. Photographic Films *Joseph H. Altman* 29.3

29.1 Glossary / *29.3*
29.2 Structure of Silver Halide Photographic Layers / *29.4*
29.3 Grains / *29.5*
29.4 Processing / *29.5*
29.5 Exposure / *29.5*
29.6 Optical Density / *29.6*
29.7 The D-Log H Curve / *29.8*
29.8 Spectral Sensitivity / *29.11*
29.9 Reciprocity Failure / *29.11*
29.10 Development Effects / *29.12*
29.11 Color Photography / *29.12*
29.12 Microdensitometers / *29.15*
29.13 Performance of Photographic Systems / *29.16*
29.14 Image Structure / *29.17*
29.15 Acutance / *29.17*
29.16 Graininess / *29.19*
29.17 Sharpness and Graininess Considered Together / *29.22*
29.18 Signal-to-Noise Ratio and Detective Quantum Efficiency / *29.22*
29.19 Resolving Power / *29.24*
29.20 Information Capacity / *29.24*
29.21 List of Photographic Manufacturers / *29.25*
29.22 References / *29.25*

Chapter 30. Photographic Materials *John D. Baloga* 30.1

30.1 Introduction / *30.1*
30.2 The Optics of Photographic Films and Papers / *30.2*
30.3 The Photophysics of Silver Halide Light Detectors / *30.7*
30.4 The Stability of Photographic Image Dyes toward Light Fade / *30.10*
30.5 Photographic Spectral Sensitizers / *30.13*

SPERO EX. 2051

30.6 General Characteristics of Photographic Films / *30.18*
30.7 References / *30.28*

Chapter 31. Image Tube Intensified Electronic Imaging *C. Bruce Johnson and Larry D. Owen* 31.1

31.1 Glossary / *31.1*
31.2 Introduction / *31.2*
31.3 The Optical Interface / *31.3*
31.4 Image Intensifiers / *31.7*
31.5 Image Intensified Self-Scanned Arrays / *31.19*
31.6 Applications / *31.27*
31.7 References / *31.30*

Chapter 32. Visible Array Detectors *Timothy J. Tredwell* 32.1

32.1 Glossary / *32.1*
32.2 Introduction / *32.2*
32.3 Image Sensing Elements / *32.2*
32.4 Readout Elements / *32.12*
32.5 Sensor Architectures / *32.21*
32.6 References / *32.35*

Chapter 33. Infrared Detector Arrays *Lester J. Kozlowski and Walter F. Kosonocky* 33.1

33.1 Glossary / *33.1*
33.2 Introduction / *33.3*
33.3 Monolithic FPAs / *33.10*
33.4 Hybrid FPAs / *33.14*
33.5 Performance: Figures of Merit / *33.23*
33.6 Current Status and Future Trends / *33.28*
33.7 References / *33.31*

Part 7. Radiometry and Photometry

Chapter 34. Radiometry and Photometry *Edward F. Zalewski* 34.3

34.1 Glossary / *34.3*
34.2 Introduction / *34.5*
34.3 Radiometric Definitions and Basic Concepts / *34.7*
34.4 Radiant Transfer Approximations / *34.13*
34.5 Absolute Measurements / *34.20*
34.6 Photometry / *34.37*
34.7 References / *34.44*

Chapter 35. Measurement of Transmission, Absorption, Emission, and Reflection *James M. Palmer* 35.1

35.1 Glossary / *35.1*
35.2 Introduction and Terminology / *35.2*
35.3 Transmittance / *35.3*
35.4 Absorptance / *35.4*
35.5 Reflectance / *35.4*
35.6 Emittance / *35.7*
35.7 Kirchhoff's Law / *35.7*
35.8 Relationship between Transmittance, Reflectance, and Absorptance / *35.7*
35.9 Measurement of Transmittance / *35.8*

SPERO EX. 2051

35.10 Measurement of Absorptance / *35.10*
35.11 Measurement of Reflectance / *35.10*
35.12 Measurement of Emittance / *35.14*
35.13 References / *35.16*
35.14 Further Reading / *35.23*

Chapter 36. Radiometry and Photometry: Units and Conversions *James M. Palmer* 36.1

36.1 Glossary / *36.1*
36.2 Introduction and Background / *36.2*
36.3 Symbols, Units, and Nomenclature in Radiometry / *36.4*
36.4 Symbols, Units, and Nomenclature in Photometry / *36.5*
36.5 Conversion of Radiometric Quantities to Photometric Quantities / *36.11*
36.6 Conversion of Photometric Quantities to Radiometric Quantities / *36.12*
36.7 Radiometric/Photometric Normalization / *36.14*
36.8 Other Weighting Functions and Conversions / *36.17*
36.9 References / *36.17*
36.10 Further Reading / *36.18*

Chapter 37. Radiometry and Photometry for Vision Optics *Yoshi Ohno* 37.1

37.1 Introduction / *37.1*
37.2 Basis of Physical Photometry / *37.1*
37.3 Photometric Base Unit—the Candela / *37.3*
37.4 Quantities and Units in Photometry and Radiometry / *37.3*
37.5 Principles in Photometry and Radiometry / *37.8*
37.6 Practice in Photometry and Radiometry / *37.11*
37.7 References / *37.12*

Chapter 38. Spectroradiometry *Carolyn J. Sher DeCusatis* 38.1

38.1 Introduction / *38.1*
38.2 Definitions, Calculations, and Figures of Merit / *38.1*
38.3 General Features of Spectroradiometry Systems / *38.7*
38.4 Typical Spectroradiometry System Designs / *38.13*
38.5 References / *38.19*

Chapter 39. Nonimaging Optics: Concentration and Illumination *William Cassarly* 39.1

39.1 Introduction / *39.1*
39.2 Basic Calculations / *39.2*
39.3 Software Modeling of Nonimaging Systems / *39.6*
39.4 Basic Building Blocks / *39.8*
39.5 Concentration / *39.12*
39.6 Uniformity and Illumination / *39.22*
39.7 Acknowledgments / *39.41*
39.8 References / *39.41*

Chapter 40. Lighting and Applications *Anurag Gupta and R. John Koshel* 40.1

40.1 Glossary / *40.1*
40.2 Introduction / *40.1*
40.3 Vision Biology and Perception / *40.3*
40.4 The Science of Lighting Design / *40.6*

SPERO EX. 2051

40.5 Luminaires / *40.24*
40.6 Lighting Measurements / *40.51*
40.7 Lighting Application Areas / *40.54*
40.8 Acknowledgments / *40.71*
40.9 References / *40.72*

Index I.1

SPERO EX. 2051

18

HIGH-BRIGHTNESS VISIBLE LEDS

Winston V. Schoenfeld

CREOL, The College of Optics and Photonics
University of Central Florida
Orlando, Florida

18.1 INTRODUCTION

Over the past decade a transformation in light emitting diode (LED) application has occurred from indicator use to the more demanding solid-state lighting and illumination markets. This includes areas such as backlighting in consumer hand-held products, outdoor displays, traffic signals, and general room lighting through the replacement of incandescent and fluorescent light sources. This transformation has been driven directly by the significant increases in LED efficiency that has enabled LEDs to penetrate into such markets. These new high-efficiency LEDs are typically referred to as high-brightness LEDs (HB-LEDs), and utilize quantum well active regions to achieve their high efficiency and lumen output.

Quantum well-active regions can have either a single quantum well (SQW) or multiple quantum well (MQW) structure, reducing internal reabsorption and increasing the radiative recombination rate of the device through greater spatial overlap of electrons and holes. A discussion of quantum wells can be found in Chap. 19, "Semiconductor Lasers." Figure 1 provides a basic structure for a modern HB-LED. It is similar to the DH structure, but utilizes a MQW active region between the *n* and *p*-type layers of the device, composed of quantum wells (QWs) that are on the order of a few nanometers in thickness. By adjusting either the composition or width of the QW, the emission wavelength of the LED can be tuned. The use of QW active regions in LEDs has not only allowed for an increase in the efficiency of the devices, it has also resulted in the ability to obtain new wavelength emissions that were not previously available due to epitaxial strain and lattice matching constraints.

18.2 THE MATERIALS SYSTEMS

There are two main semiconductor material systems currently exploited for visible HB-LEDs. These are the AlInGaP and AlInGaN systems. A detailed discussion of the AlInGaP system is in Chap. 17, "Light-Emitting Diodes." AlInGaP is used for amber and red LEDs that fall within the 590- to 650-nm wavelength region. It is limited to this wavelength range because the AlInGaP quaternary shifts to an indirect band gap as wavelengths below 590 nm are targeted. This left a void in the blue and green spectral regions for visible HB-LEDs.

SPERO EX. 2051

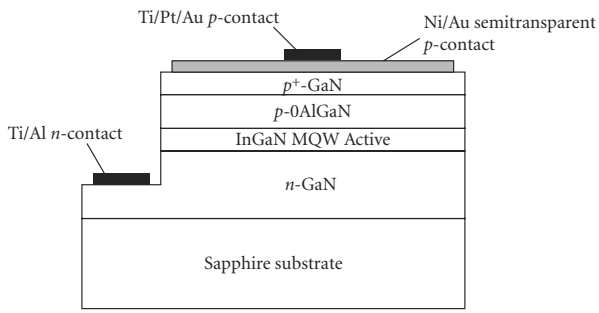

FIGURE 1 Typical structure for a modern InGaN HB-LED showing associated epitaxial layers, including the multiquantum well (MQW) active region.

In the past decade, this void has been quickly filled with MQW LEDs made from the AlInGaN material system. GaN has a wurtzite crystal structure and band gap at room temperature of about 3.2 eV (385 nm). By alloying with Al or In, the band gap can be shifted to shorter or longer wavelengths, respectively. This has led to the realization of InGaN QW active regions in HB-LEDs offering light output in the blue to green spectral regions. Although InN has a direct energy gap of 0.7 eV, phase segregation in InGaN alloys limits the ability to obtain active regions emitting at wavelengths above 530 nm. Despite this, InGaN QW active regions have successfully been used to create blue and green HB-LEDs with complete wavelength tunability across the visible 400- to 530-nm range.

18.3 SUBSTRATES AND EPITAXIAL GROWTH

Current AlInGaN HB-LEDs use one of two substrates: sapphire or silicon carbide (SiC). Despite considerable lattice mismatch between these and GaN (roughly 16 percent for sapphire and 3.5 percent for SiC), low-temperature buffer layer technologies have been developed to allow for nucleation and growth of high-quality AlInGaN HB-LEDs. Low-temperature AlN buffer layers on sapphire substrates are directly formed by MOCVD that result in dislocation entanglement just above the nucleation interface. As depicted in Fig. 2, many of the dislocations interact and annihilate. The subsequent growth of a thick (typically 3 to 4 μm) *n*-GaN buffer layer further reduces dislocation density below 10^9 per cm^2. The use of 6H-SiC substrates offers closer lattice matching and lower defect densities, although this comes with a higher cost that has kept sapphire as a more popular substrate solution. Recent research has aimed to produce native or lattice-matched substrate solutions for GaN growth. Native GaN substrates have been produced, although the diameter of such substrates and cost remain a challenge. A sister wide band gap compound, ZnO, has strikingly similar properties

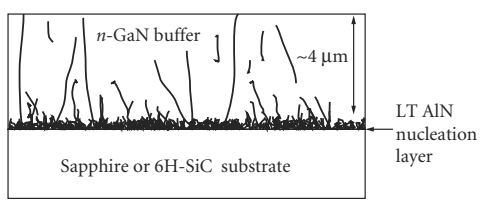

FIGURE 2 Cross-section schematic of the dislocation reduction that occurs due to use of a low temperature (LT) AlN nucleation layer. Dislocations originate from the large lattice mismatch of the nitrides with SiC or sapphire substrates, but can be reduced well below $10^9/cm^2$ when a LT-AlN nucleation layer and thick GaN buffer layer are used.

SPERO EX. 2051

to GaN and is currently considered a good candidate for a lattice matched substrate for AlInGaN HB-LED growth. ZnO has the same wurtzite crystal structure as GaN, is nearly lattice matched to GaN, and can be easily doped *n*-type to form a conductive substrate. Lattice matched substrates made from ZnO have just become commercially available through hydrothermal growth.

Growth of AlInGaN HB-LEDs is accomplished commercially with MOCVD (a short discussion of MOCVD was provided in Sec. 17.8 in Chap. 17). While high quality growth of AlInGaN epitaxial films has been demonstrated by MBE, typical HB-LED structures require 4- to 5-μm-thick films that are not economically realizable in MBE systems due to the slow growth rate and limited number of substrates per growth. MOCVD reactors are able to accommodate multiple 2″ substrates per growth (as many as 40 in larger systems) with the necessary uniformity and control of film thickness. One of the initial challenges in AlInGaN HB-LED growth was *p*-type doping of GaN. The metal-organic precursor sources of MOCVD introduce a considerable amount of hydrogen into the films that directly compensates *p*-type acceptors. This issue was resolved through post-growth annealing at temperatures above 800°C in which the excess hydrogen is driven out of the epitaxial films. Upon out-diffusion of the hydrogen, the *p*-type acceptors become active and the necessary hole injection into the structures is then possible.

18.4 PROCESSING

Many of the steps covered in Sec. 17.9 of Chap. 17 are used in the fabrication of HB-LED epitaxial wafers. Sapphire substrates are electrically insulating, imposing the need for creating both *n*- and *p*-type contacts on the front of the HB-LED surface as was shown in Fig. 1. As a result, the epitaxial structure must be etched down to the *n*-GaN layer in order to make electrical contact to the *n*-side of the HB-LED structure. AlInGaN is relatively resistant to wet chemical etching and must be dry etched using reactive ion etching (RIE) or inductively coupled plasma (ICP) methods. RIE/ICP is capable of high etch rates that are anisotropic, meaning that they are capable of etching vertically down into the structure with little to no lateral etching. SiC substrates are electrically conductive and thus allow for the *n*-contact to be formed on the back side of the substrate without the need for etching of the front surface.

The typical fabrication process for AlInGaN HB-LEDs utilizes four lithographic steps. These include the mesa etch, SiO_2 passivation, *n*-contact, and *p*-contact layers. A top view and associated cross section of a standard HB-LED device are given in Fig. 3, indicating these layers. Prior to the

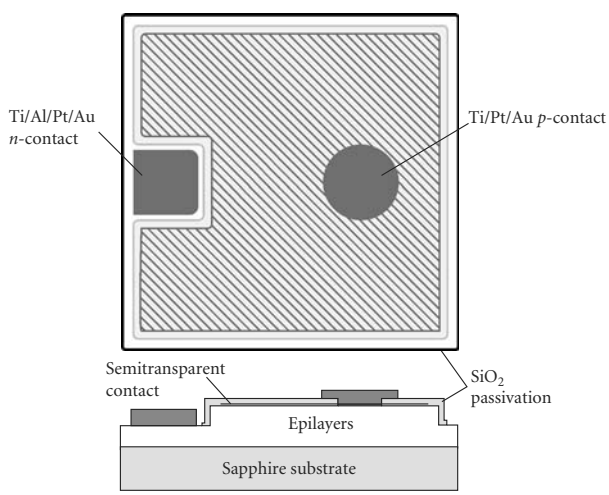

FIGURE 3 Top view and cross-section schematic of a standard nitride HB-LED. A mesa is etched to allow for contact to the *n*-type underlayer. A semitransparent contact on top of the mesa is used to promote uniform hole injection due to poor hole mobility in the *p*-GaN.

SPERO EX. 2051

first lithographic step a semitransparent top contact is deposited on the surface (*p*-side) of the entire epi wafer. This is necessary in order to achieve uniform current injection across the device due to the higher resistivity of the *p*-GaN in comparison to the *n*-GaN. The most common semitransparent contacts are Ni/Au and indium tin oxide (ITO), with Ni/Au being the most widely used. Once the semitransparent contact is formed the lithographic steps are then carried out. The mesa etch is a dry etch step to access the *n*-GaN layers for the *n*-type contact as required when using sapphire substrates. The SiO_2 passivation step covers the side walls of the mesa and protects its lateral edges. Once the passivation is in place, the last two lithographic steps define the *n*- and *p*-type contacts to the device through a lift-off process. Common metallizations are Ti/Al/Pt/Au for the *n*-contact and Ti/Pt/Au for the *p*-contact to the semitransparent contact underlayer. To separate the individual LEDs on the fabricated wafer, the substrate must first be thinned from its typical 400 μm thickness to on the order of 80 to 100 μm using a multiple step wafer polishing method on automated multiwafer polishers. Once thinned, singulation of the individual die is accomplished either by a scribe and break method or by using laser separation. The sawing method typically employed for other III–V LEDs is not possible due to the substantial hardness of sapphire and SiC that greatly limits their ability to be cut using a dicing saw.

18.5 SOLID-STATE LIGHTING

The current push towards energy conservation has created a considerable interest in the replacement of conventional lighting by solid-state LED fixtures. LEDs offer the potential to considerably reduce power consumption while maintaining the necessary lumen output for lighting. Generating white light from HB-LEDs is typically accomplished by one of two methods as depicted in Fig. 4. The first method, shown in Figs. 4*a* and *b*, utilizes an AlInGaN-LED in conjunction with one or more phosphors. When a UV-LED is used, the UV light emission is absorbed and re-emitted by a mixture of red, green, and blue phosphors. As indicated in Fig. 4*a* the phosphors down-convert the UV light (dashed line) to visible light (solid line), and when the appropriate ratio of phosphors is used, white light is emitted. A more common LED/phosphor combination used for general illumination is the combination of a blue (~465 nm) AlInGaN-LED and a yttrium aluminum garnet (YAG) phosphor such as cerium doped $Y_3Al_5O_{12}$. In this approach (Fig. 4*b*) a portion of the blue LED emission is absorbed by the YAG phosphor and down-converted to the yellow spectral region. When the proper ratio of YAG phosphor is used, the resulting binary complimentary output of the blue LED and yellow YAG phosphor creates white light as perceived by observers. The second method for white light emission is preferred when color tuning is necessary, such as in outdoor displays. As indicated in Fig. 4*c*, by using red, green, and blue LEDs, one can create white light when the appropriate ratio of each is selected. This RGB approach has the added benefit of allowing the user to create any color within the associated color gamut by balancing the ratio of the individual LEDs.

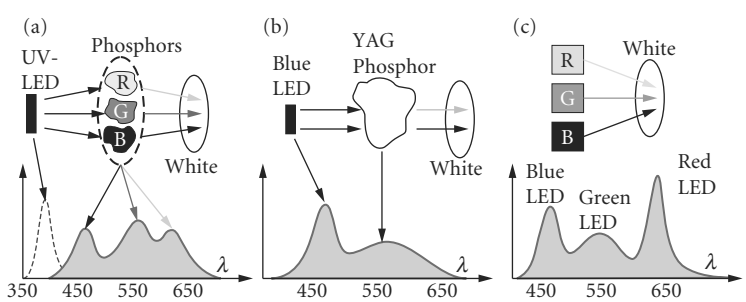

FIGURE 4 Methods for white light generation using HB-LEDs. White light is achieved by using a HB-LED and phosphors (*a* and *b*), or the combination of a red, green, and blue HB-LED (*c*).

SPERO EX. 2051

This method also allows for active adjustment of the color temperature of white light emission which is not possible using the LED/phosphor approach.

The primary figure of merit for solid-state lighting is the luminous efficacy of the fixture. Luminous efficacy refers to the ratio of lumen output from the source to the power input, and has the units of lumens per Watt (lm/W). Conventional incandescent and fluorescent lights have typical luminous efficacies of 15 lm/W and 70 lm/W, respectively, varying somewhat depending on manufacturer. As of early 2008, currently available LED-based replacements have luminous efficacies as high as 80 lm/W, exceeding compact fluorescents. By comparison, lab demonstrations of white LEDs are commonly breaking 120 lm/W, with the expectation of reaching 150 lm/W in the near future. Despite these accomplishments the added cost of solid-state white lighting has slowed the market acceptance. A common cost comparison is the first cost of a light source, typically measured in terms of the cost per kilolumen (klm). Incandescent and fluorescent light sources fall in the $0.5 to $3.00 per klm, while current light emitting diode sources fall easily in the $20 to $30 per klm range. Considerable progress in efficiency continues to climb and it is expected that as the luminous efficacy and lifetime of solid-state white LEDs continues to rise that the cost per kilolumen will decrease while market acceptance increases.

18.6 PACKAGING

HB-LEDs chips for standard current use (20 to 70 mA) have lateral geometries on the order of $350 \times 350\ \mu m^2$. Such LED chips are commonly packaged similarly to IR-LEDs in a 5-mm T1-3/4 format, as shown in Figs. 21 and 22 in Chap. 17. For AlInGaP HB-LEDs the substrate is conductive and silver filled epoxy is used for attaching the die to the lead frame to form one of the contacts. The other contact is formed using standard ball wire bonding to the top of the LED chip. For AlInGaN HB-LEDs, commonly grown on insulating sapphire substrates, two wire bonds are required to make the electrical connections to the lead frame. Silver-filled epoxy is still used for such LEDs since the sapphire is transparent and emission can be effectively redirected upward from the epoxy surface below the chip. In addition to the 5-mm T1-3/4 package, a considerable number of new surface mount device (SMD) packages have become available to support the introduction of HB-LEDs into the consumer hand-held device market. A schematic of a typical SMD package is provided in Fig. 5. The LED is placed on a metal lead frame that is encased in a plastic outer shell. Once the HB-LED has been die bonded into the package with silver-filled epoxy, it is then wire bonded and encapsulated with transparent epoxy for protection. Such SMD packages are typically several millimeters on a side; however, smaller versions with formats nearly identical to chip resistors are available that have

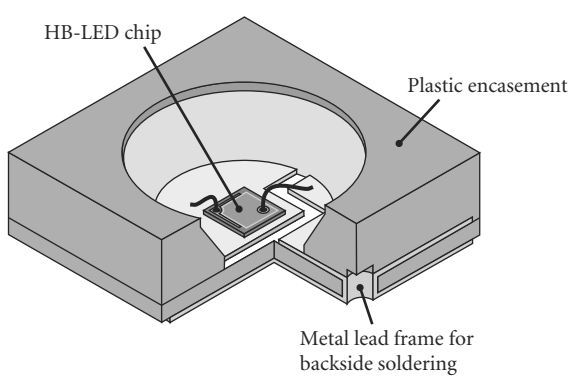

FIGURE 5 Schematic of a standard surface mount device (SMD) package for HB-LEDs.

SPERO EX. 2051

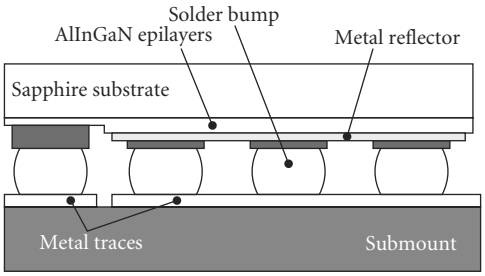

FIGURE 6 Cross-section schematic of the flip chip geometry used for high-power nitride LEDs. Flip chip packaging allows for increased heat dissipation from the LED junction, enabling them to be driven at much higher current densities.

very small form factors providing the low profile necessary for applications such as cell phone key pad backlighting.

In recent years the push for solid-state white lighting has resulted in a transition to larger HB-LED chip sizes and an increase in the operating current densities. The latter brings new constraints to packaging due to the increased need for thermal management in an effort to keep the junction temperature of the HB-LED as low as possible. While the traditional packaging formats have proven very effective for standard drive current use, they are not suitable for high drive current applications using large area HB-LEDs since they do not provide adequate thermal management. This has forced a significant change in not only the design of packaging for high drive current, large area HB-LEDs, but also the devices themselves. Most HB-LEDs use sapphire substrates that provide very poor heat dissipation from the LED junction due to the low thermal conductivity of sapphire. This has been overcome by using a flip chip approach, where the LED chip is flipped over onto a carrier and attached using solder bump methods similar to the silicon IC industry. A rough schematic of a flip chip geometry is shown in Fig. 6. The HB-LED chip is designed to support multiple solder bump attachments to the submount. A highly reflective metal layer is formed on the *p*-side of the device to redirect light emission through the backside of the device. The solder bumps affix the LED die firmly to the submount and create the electrical connections to the metal traces below, allowing for subsequent wire bonding between the submount and the external leads of the package. The solder bumps also serve as a route for efficient heat transfer from the LED junction to the submount enabling the junction temperature of the LED chip to remain low under high drive current conditions. There are a variety of external package geometries that have been developed to support flip chip HB-LEDs with no specific convention between manufacturers. Among the main considerations in the package design has been the encapsulant around the LED and providing a low thermal resistance path to the external housing. Standard clear epoxies that are used in conventional packages typically cannot withstand temperatures much above 100°C. In flip chip high drive packages this can be easily exceeded and would cause thermal damage to conventional epoxies. This has led many companies to develop a variety of new high-index encapsulants, such as silicones, that are able to withstand the higher temperature demands of high drive solid-state lighting. Low thermal resistance packaging has also followed many new routes such as packages with copper tungsten metal bases, metal core board, and high thermal conducting insulating materials (e.g., BeO and AlN).

SPERO EX. 2051

- Location (latitude and longitude) and orientation of the building relative to the surroundings. Simulating the daylight entering the building during various times of the day and the year.
- Design for reduction or elimination of glare from daylight sources. Internal layout of the building during intended use will play a key role.
- Outside view requirements via windows. A minimum window size[61–63] is needed for a given geographic location, and a certain window location is dictated by aesthetic reasons including the desired view from the window. The minimum window size can also depend upon the prevalent building regulations based on wall size or floor size. Under such circumstances, the daylight entering must be controlled or balanced with interior lighting and cooling for uniformity, glare, and heat management. Daylight can be controlled by providing appropriate window shades, glazings, or even additional windows or skylights at appropriate places.

It is not always possible to obtain energy savings with daylight due to increased heat load, especially during summers and the need to supplement daylight with electrical lighting during the night. Infrared rejection is achieved by using special glazings. To limit glare, glazing such as high reflectance, low transmittance, electrically controlled transmission, tilted glazings with angularly dependent transmittance or IR reflecting films are used. Adequate consideration must be given to the window view impact due to any of the daylight control mechanisms. A very low-transmittance glazing can make the outside view appear gloomy on a bright day.

Luminaire Design

The source is the starting point of the luminaire design. The optics performs at a minimum two functions: first to capture the light from source and second to transfer light efficiently to the desired distribution at the target (i.e., illuminance, intensity, and/or luminance). The choice of the optics is also a challenging process. First, the designer must select if refractive, reflective, or both types of optics (i.e., hybrid) are to be used in the design. Reflective optics have been a standard for most sources, with flat refractive optics used at the output aperture in order to protect the other optics. Until recently reflectors were standard conics such as ellipses, hyperbolas, parabolas, or spheres. Standard refractors in use include cover plates (still called a lens), pillow lens arrays, Fresnel lenses, and other faceted designs. However, with advances in LEDs, refractive optics are increasingly being used for advanced function. Solid-state lighting optics are either plastic or glass that surround individual or a limited number of LEDs. They are hybrid optics that use at least total internal reflection (TIR) and refraction at the input and output facets, but they can also use reflection, scattering, and even diffraction. With the advent of better technology, especially manufacturing capabilities and software for modeling, faceted and continuously smooth surfaces parameterized with nonuniform rational B-splines (NURBS) are being developed. For high-performance, injection molding of plastic or glass is being increasingly used. For refractive optics, the surfaces are left bare, but for reflective optics there is vacuum metallization of the surfaces. Reflectors are also made with stamping methods, but these optics tend to have lower performance.

Baffles (louvers) are often considered by many to be optics of the system; however, many, rather than shaping a distribution through redirection of the light, block or even absorb incident radiation. Thus, while some baffles are reflective and provide some shaping of the illumination distribution, they most often achieve shaping through subtraction rather than addition. They are primarily added to alleviate glare, trespass, and pollution, but they are also included for aesthetic reasons, correcting errors in the design process, and to hide structure within the luminaire.

The source coupling aspect is the focus of the next section, following that is a discussion of the design of the optics and subsections on baffling in the form of luminaire cutoff classification and types of luminaires. Following this process from the source to the optics to the baffle to the target, while always considering the perception aspects of the illumination (see Sec. 40.3), means that aesthetically pleasing while technically sound lighting can be developed.

Étendue and Source Coupling For reflective optics, the source-coupling components also act as the transfer optics, often in conjunction with a front, protective lens. With the advances in source

SPERO EX. 2051

technology that use hybrid, dielectric components, coupling of the sources, is increasingly important in order to improve upon system efficiency. Typically, individual LEDs are placed in recesses in the dielectric optic, and by obeying the conditions for TIR, all of the emitted light can be captured by the coupler and then transferred to following optics that shape the emitted distribution.

In all cases, the term étendue describes the flux transfer characteristics of the optics, starting with the coupling optics, of an optical system, such as a luminaire. Étendue is a geometrical quantity that is the integrated product of an area and solid angle. In paraxial form it is the Lagrange Invariant, but in nonparaxial form it is given by

$$\mathscr{E} = n^2 \iint_{\text{pupil}} \cos\theta dA d\Omega \tag{12}$$

where $\mathscr{E}$ is the étendue, dA is the differential area, $d\Omega$ is the differential solid angle, θ is the angle with respect to the surface of interest (i.e., normal), and n is the index of refraction of the space. The limits of integration in area are over some aperture (e.g., a lens clear aperture or a reflector exit aperture), while the solid angle integration is over the limits that are passed by the aperture. For example, consider a source of area A_s that emits into a half angle of θ_0 from every point on the surface. The étendue for this source is

$$\mathscr{E} = n^2 A_s \int_0^{2\pi} \int_0^{\theta_0} \cos\theta \sin\theta d\theta d\phi = \pi n^2 A_s \sin^2\theta_0 \tag{13}$$

In lossless optical systems, étendue is conserved. Thus, in order to design the most efficient luminaire, one must continue to match the étendue as one progresses through the optical components of the system. For example, if the source of Eq. (13) is used for a luminaire, one must keep this étendue quantity consistent. If one desires to reduce the angular spread of the output from an optic ($\theta_0 > \theta_{\text{optic}}$), then the area of the optic must be increased ($A_s < A_{\text{optic}}$). The counter also holds true: to reduce the real extent ($A_s > A_{\text{optic}}$), one must increase the angle ($\theta_0 < \theta_{\text{optic}}$). An expression for conservation of étendue in a generalized form is

$$dx\,dy\,dp\,dq = dx'\,dy'\,dp'\,dq' \tag{14}$$

where the dx and dy terms are the differential position terms and the dp and dq terms are the differential optical direction cosine terms, which are equivalent to ndL and ndM respectively. More information about étendue can be found in Chap. 39, "Nonimaging Optics: Concentration and Illumination," in this volume. Another factor related to étendue through a differential is skewness, which denotes the twist on individual rays of light in an optical system. Skewness is also invariant and implies that transfer from one source geometry (e.g., a square) cannot be transformed to another source geometry (e.g., a circle) without loss except if some rotational asymmetry is added to the optical system. Further information about étendue and associated terms like skewness can be found in the literature.[64]

Luminaire Design Methods There are a multitude of design principles for the design of the optics of a luminaire. Fundamentally, most design methods are based on the basic conic shapes as listed in Table 6. Each of these shapes provides a basic intensity distribution at its output aperture. However, increasing demands of tailored light distributions and also increased efficiency require perturbations to these basic design forms. Furthermore, the topics of light trespass, light pollution, and glare are receiving a wealth of attention from ordinance and regulatory agencies. To reduce glare issues it is best to use diffuse optics with a well-defined cutoff. In the field of nonimaging optics (see Chap. 39), the edge-ray theorem provides a means to have a well delineated cutoff. The edge ray is defined by the maximum extent of the source, thus providing a maximum cone of light from the reflector designed around the source shape. However, the edge-ray principle is passive with respect to the luminance distribution of the source—it contends for the maximum extents but not the physical distribution of light in the radiation pattern.

Thus, tailoring methods have been developed. The tailoring methods specify the shape of the optics based upon the luminance distribution of the source and the desired illumination pattern

SPERO EX. 2051

TABLE 6 Basic Conic Shapes, Their Conic Provide at Their Output Aperture Constant, and the Basic Intensity Distribution That They Provide at Their Output Aperture

Shape	Conic Constant (k)	Base Intensity Distribution
Hyperbolic	$k < -1$	Diverging; far-field applications
Parabolic	$k = -1$	Collimating; pseudocollimation applications
Elliptic	$-1 < k < 0$	Converging; near-field applications
Spheric	$k = 0$	Converging; self-imaging applications

(i.e., luminance, illuminance, and/or intensity) at the target. These methods are extensive and beyond the confines of this chapter. The reader is encouraged to consult the *Handbook* chapter on nonimaging optics (Chap. 39) for a brief introduction, the theoretical book on nonimaging optics by Winston, Miñano, and Benítez,[64] and the applied book on nonimaging optics by Chaves.[65]

Luminaire Cutoff Classification A cutoff ensures that light from the luminaire is restricted above the horizon with respect to the lamp geometry. Cutoff is designed into the luminaire through the optics (i.e., edge-ray designs) and/or the integration of baffles. While most applications do not require cutoff classification, except for those used on the exterior, such as automotive, roadway, and landscape lighting, most designers include such to make effective lighting systems by alleviating potential glare, trespass, and pollution concerns. Often strict cutoff guidelines are mandated by governmental standards, such as for automotive, traffic signal, and roadway lighting. The goals are to provide the required lighting level to its users, while also alleviating light pollution and light trespass. Light pollution is light that is directed up into the atmosphere, causing sky glow, which is especially present in urban settings. The reduction of light pollution is a growing trend being addressed by the astronomy community. When light is incident on surfaces outside the intended illumination region, it is called *light trespass*. The impact of light trespass from roadway lighting is a major concern in residential areas.

For both trespass and pollution the luminaire cutoffs provide a protocol to reduce both. Automotive lighting does not use the criteria presented here, but rather use a set of governmental standards. Roadway and external lighting make the most use cutoff criteria as shown in Table 7. See Fig. 22 for a depiction of the angles listed in Table 7.[66]

Luminaire Classification System In 2007 the IESNA published research results for refinement of the cutoff classification system of the previous section.[67] This study focused on light distribution in front of the luminaire (forward light), behind the luminaire (back light), and above the luminaire (uplight) as shown in Fig. 21. They found the photometric luminaire efficiency ($\eta_{\text{luminaire}}$) to be

$$\eta_{\text{luminaire}} = 100\frac{\Phi_{\text{forward}} + \Phi_{\text{back}} + \Phi_{\text{uplight}}}{\Phi_{\text{source}}} \tag{15}$$

where Φ_{forward}, Φ_{back}, Φ_{uplight}, and Φ_{source} are the integrated fluxes in lumens over the solid angles shown in Fig. 21 for forward light, back light, uplight, and the bare source, respectively.

TABLE 7 Amount of Emitted Light Criteria for the Luminaire Cutoff Classification[66]

Type	Horizon and above (90° and greater)	10° below Horizon (80° to 90°)	Remainder (0° to 80°)
Full Cutoff	0%	≤10%	≥90%
Cutoff	<2.5%	≤10%	≥87.5%
Semicutoff	<5%	≤20%	≥75%
Noncutoff	No restrictions over entire angular space		

SPERO EX. 2051

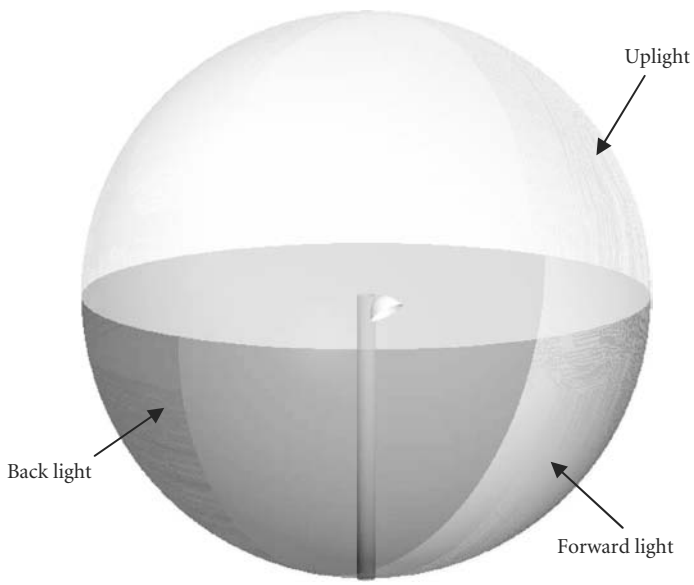

FIGURE 21 Lighting classification system zones for forward light, back light, and uplight based upon the exit aperture of the luminaire.

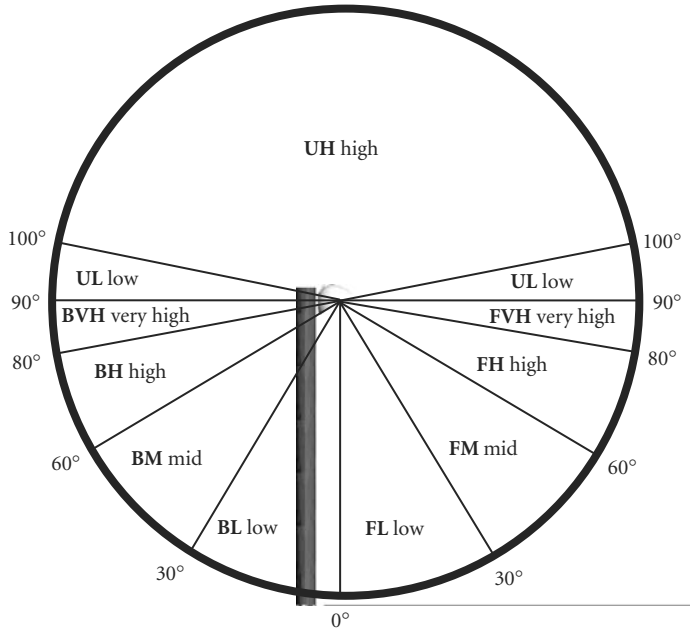

FIGURE 22 Layout of the light classification system subzones. (See also color insert.)

SPERO EX. 2051

These three zones are then broken down into a total of 10 subzones as shown in Fig. 22. The lumens in each subzone is measured with respect to the bare source flux, as in Eq. (15), in each of these subzones and then reported as an evaluation of the luminaire. These subzones indicate the distribution of light over several regions rather than restricted to the 80° and greater as per the previous section. Standard goals include reduction of light above the horizon (i.e., all uplight subzones and the BVH and FVH subzones) and the desired uniformity over the other zones. This new classification system provides for better control of the illumination such that both vertical and horizontal surface illuminances can be addressed in the design process. Horizontal surface illuminance criteria are met by increasing the flux in the BM to FM subzones. Vertical surface illuminance criteria are met by increasing the flux in the BM, BH, FM, and FH subzones.

Luminaire Optics There are innumerable schemes to the design and availability of luminaire optics, both for artificial and natural sources. Methods employing reflectors, refractors, TIR optics, and combinations thereof have been developed. Additionally, the optics are both specular and diffuse or a combination of these two are used. In the next few subsections, we provide examples of commonly available luminaire optics. Finally, as per Table 6, the shapes of the optics are typically based on conic shapes.

Luminaire optics for artificial sources While the design of the optics of the luminaire is to provide a desired illumination distribution, we learned from the previous sections that light cutoff is important in the design of the luminaire. In fact, the ability to hide or shield the source from direct view in order to reduce glare concerns is as equally important as obtaining the desired illumination distribution. A reflector as shown in Fig. 23*a* has a fairly wide direct view of the source, denoted as the shielding angle or similarly the cutoff angle. Room lamps are perfect examples of this dual requirement since it is typical to use a diffuse shade around the source. The source and shade (which also acts as a diffuse reflector) provide the desired general illumination, while the shade provides the requisite cutoff. Besides using the body of the reflector to hide the direct view of the source, louvers or baffles (see Fig. 23*b*), a prismatic or Fresnel lens (see Fig. 23*c*), or a bulb shield (see Fig. 23*d*) are

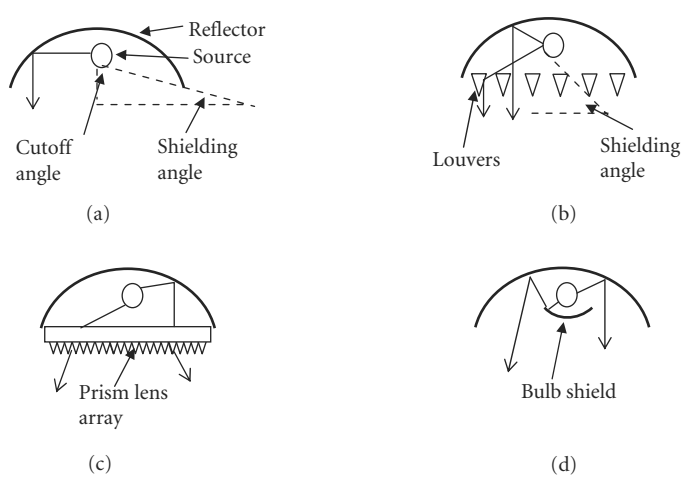

FIGURE 23 Glare issues of four luminaire geometries: (*a*) the reflector providing the cutoff; (*b*) louvers, flat or parabolic, increasing the shielding angle; (*c*) a lens array, prismatic or Fresnel, which directs more of the light emission downward thus reducing the direct intensity level of the source; and (*d*) the inclusion of a bulb shield to ensure that all emission strikes the primary reflector at least once. (*Adapted from Ref. 5, p. 71.*)

SPERO EX. 2051